

Evidence for $B \rightarrow K\eta'\gamma$ Decays at Belle

R. Wedd,²¹ I. Adachi,⁸ H. Aihara,⁴¹ K. Arinstein,^{1,31} V. Aulchenko,^{1,31} A. M. Bakich,³⁸ V. Balagura,¹² E. Barberio,²¹ A. Bay,¹⁸ K. Belous,¹¹ V. Bhardwaj,³³ M. Bischofberger,²³ A. Bondar,^{1,31} A. Bozek,²⁷ M. Bračko,^{20,13} T. E. Browder,⁷ Y. Chao,²⁶ A. Chen,²⁴ B. G. Cheon,⁶ I.-S. Cho,⁴⁵ Y. Choi,³⁷ J. Dalseno,⁸ M. Dash,⁴⁴ A. Drutskoy,³ S. Eidelman,^{1,31} D. Epifanov,^{1,31} N. Gabyshev,^{1,31} P. Goldenzweig,³ H. Ha,¹⁶ Y. Horii,⁴⁰ Y. Hoshi,³⁹ W.-S. Hou,²⁶ H. J. Hyun,¹⁷ T. Iijima,²² K. Inami,²² A. Ishikawa,³⁴ R. Itoh,⁸ M. Iwasaki,⁴¹ D. H. Kah,¹⁷ N. Katayama,⁸ H. Kawai,² T. Kawasaki,²⁹ H. O. Kim,¹⁷ J. H. Kim,³⁷ Y. I. Kim,¹⁷ Y. J. Kim,⁵ K. Kinoshita,³ B. R. Ko,¹⁶ P. Križan,^{19,13} P. Krokovny,⁸ T. Kuhr,¹⁵ R. Kumar,³³ A. Kuzmin,^{1,31} Y.-J. Kwon,⁴⁵ S.-H. Kyeong,⁴⁵ M. J. Lee,³⁶ S.-H. Lee,¹⁶ T. Lesiak,^{27,4} J. Li,⁷ A. Limosani,²¹ C. Liu,³⁵ D. Liventsev,¹² R. Louvot,¹⁸ A. Matyja,²⁷ S. McOnie,³⁸ H. Miyata,²⁹ R. Mizuk,¹² T. Mori,²² Y. Nagasaka,⁹ M. Nakao,⁸ H. Nakazawa,²⁴ Z. Natkaniec,²⁷ S. Nishida,⁸ O. Nitoh,⁴³ T. Ohshima,²² S. Okuno,¹⁴ H. Ozaki,⁸ P. Pakhlov,¹² G. Pakhlova,¹² C. W. Park,³⁷ H. K. Park,¹⁷ K. S. Park,³⁷ R. Pestotnik,¹³ L. E. Piilonen,⁴⁴ A. Poluektov,^{1,31} H. Sahoo,⁷ Y. Sakai,⁸ O. Schneider,¹⁸ J. Schümann,⁸ K. Senyo,²² M. E. Sevier,²¹ M. Shapkin,¹¹ V. Shebalin,^{1,31} J.-G. Shiu,²⁶ B. Shwartz,^{1,31} J. B. Singh,³³ A. Sokolov,¹¹ S. Stanič,³⁰ M. Starič,¹³ K. Sumisawa,⁸ T. Sumiyoshi,⁴² S. Suzuki,³⁴ G. N. Taylor,²¹ Y. Teramoto,³² K. Trabelsi,⁸ S. Uehara,⁸ Y. Unno,⁶ S. Uno,⁸ P. Urquijo,²¹ Y. Usov,^{1,31} G. Varner,⁷ K. E. Varvell,³⁸ K. Vervink,¹⁸ A. Vinokurova,^{1,31} C. H. Wang,²⁵ M.-Z. Wang,²⁶ P. Wang,¹⁰ Y. Watanabe,¹⁴ J. Wicht,⁸ E. Won,¹⁶ B. D. Yabsley,³⁸ H. Yamamoto,⁴⁰ Y. Yamashita,²⁸ Z. P. Zhang,³⁵ V. Zhilich,^{1,31} V. Zhulanov,^{1,31} T. Zivko,¹³ A. Zupanc,¹³ and O. Zyukova^{1,31}

(The Belle Collaboration)

¹*Budker Institute of Nuclear Physics, Novosibirsk*²*Chiba University, Chiba*³*University of Cincinnati, Cincinnati, Ohio 45221*⁴*T. Kościuszko Cracow University of Technology, Krakow*⁵*The Graduate University for Advanced Studies, Hayama*⁶*Hanyang University, Seoul*⁷*University of Hawaii, Honolulu, Hawaii 96822*⁸*High Energy Accelerator Research Organization (KEK), Tsukuba*⁹*Hiroshima Institute of Technology, Hiroshima*¹⁰*Institute of High Energy Physics, Chinese Academy of Sciences, Beijing*¹¹*Institute of High Energy Physics, Protvino*¹²*Institute for Theoretical and Experimental Physics, Moscow*¹³*J. Stefan Institute, Ljubljana*¹⁴*Kanagawa University, Yokohama*¹⁵*Institut für Experimentelle Kernphysik, Universität Karlsruhe, Karlsruhe*¹⁶*Korea University, Seoul*¹⁷*Kyungpook National University, Taegu*¹⁸*École Polytechnique Fédérale de Lausanne (EPFL), Lausanne*¹⁹*Faculty of Mathematics and Physics, University of Ljubljana, Ljubljana*²⁰*University of Maribor, Maribor*²¹*University of Melbourne, School of Physics, Victoria 3010*²²*Nagoya University, Nagoya*²³*Nara Women's University, Nara*²⁴*National Central University, Chung-li*²⁵*National United University, Miao Li*²⁶*Department of Physics, National Taiwan University, Taipei*²⁷*H. Niewodniczanski Institute of Nuclear Physics, Krakow*²⁸*Nippon Dental University, Niigata*²⁹*Niigata University, Niigata*³⁰*University of Nova Gorica, Nova Gorica*³¹*Novosibirsk State University, Novosibirsk*³²*Osaka City University, Osaka*³³*Panjab University, Chandigarh*³⁴*Saga University, Saga*³⁵*University of Science and Technology of China, Hefei*³⁶*Seoul National University, Seoul*³⁷*Sungkyunkwan University, Suwon*

³⁸University of Sydney, Sydney, New South Wales

³⁹Tohoku Gakuin University, Tagajo

⁴⁰Tohoku University, Sendai

⁴¹Department of Physics, University of Tokyo, Tokyo

⁴²Tokyo Metropolitan University, Tokyo

⁴³Tokyo University of Agriculture and Technology, Tokyo

⁴⁴IPNAS, Virginia Polytechnic Institute and State University, Blacksburg, Virginia 24061

⁴⁵Yonsei University, Seoul

We present the results of a search for the radiative decay $B \rightarrow K\eta'\gamma$ and find evidence for $B^+ \rightarrow K^+\eta'\gamma$ decays at the 3.3 standard deviation level with a partial branching fraction of $(3.6 \pm 1.2 \pm 0.4) \times 10^{-6}$, where the first error is statistical and the second systematic. This measurement is restricted to the region of combined $K\eta'$ invariant mass less than $3.4 \text{ GeV}/c^2$. A 90% confidence level upper limit of 6.4×10^{-6} is obtained for the decay $B^0 \rightarrow K^0\eta'\gamma$ in the same $K\eta'$ invariant mass region. These results are obtained from a 605 fb^{-1} data sample containing $657 \times 10^6 B\bar{B}$ pairs collected at the $\Upsilon(4S)$ resonance with the Belle detector at the KEKB asymmetric-energy e^+e^- collider.

PACS numbers: 13.25.Hw, 13.20.He, 14.40.Gx, 14.40.Nd

Radiative B meson decays proceed primarily through the flavour changing neutral current (FCNC) quark-level process $b \rightarrow s\gamma$. FCNC processes are forbidden at tree-level within the Standard Model (SM), and hence $b \rightarrow s\gamma$ must proceed via radiative loop diagrams. As loop processes may include unknown heavy particles mediating the loop, any disparity between experimental measurement and SM prediction could be evidence of such new particles.

The world average experimental branching fraction (BF) for the meson-level process $B \rightarrow X_s\gamma$ ($(3.55 \pm 0.26) \times 10^{-4}$ [1]) and the theoretical SM predictions ($(3.15 \pm 0.23) \times 10^{-4}$ [2]) are consistent. Measurements of individual exclusive $B \rightarrow X_s\gamma$ modes, such as $B \rightarrow K\eta'\gamma$, provide consistency checks on the agreement between theory and experiment, and improve our understanding of the hadronization process in $B \rightarrow X_s\gamma$ and $B \rightarrow X_sl^+l^-$.

The analysis of the decay mode $B \rightarrow K\eta'\gamma$ uses 605 fb^{-1} of data collected at the $\Upsilon(4S)$ resonance with the Belle detector. This decay was previously studied by BABAR who set upper limits (ULs) of $\mathcal{B}(B^+ \rightarrow K^+\eta'\gamma) < 4.2 \times 10^{-6}$ and $\mathcal{B}(B^0 \rightarrow K^0\eta'\gamma) < 6.6 \times 10^{-6}$ at 90% confidence level (CL) from an analysis of 211 fb^{-1} of data [3].

A previous comparison of the modes $B \rightarrow K\eta$ and $B \rightarrow K\eta'$ showed a surprising suppression of the former with respect to the latter, due to destructive interference between two penguin amplitudes [4]. The ability of QCD factorization techniques to correctly predict this BF hierarchy has been demonstrated, though the errors are large [5]. A similar comparison of the observed $B \rightarrow K\eta\gamma$ mode [6][3] and the previous upper limits for $B \rightarrow K\eta'\gamma$ shows the opposite trend for these BF's. The analogous QCD calculation has not yet been performed for these decay modes. Measurement of $B \rightarrow K\eta'\gamma$ is an important test of such a calculation. In addition, a time-dependent charge-parity (CP) asymmetry measurement will be possible if there are sufficient statistics for the decay $B^0 \rightarrow K_S^0\eta'\gamma$ [7]. Such mixing-induced CP asymmetries are suppressed within the SM, but some beyond-SM theories involving right-handed currents allow them to be large, even when the $B^0 \rightarrow K_S^0\eta'\gamma$ BF agrees with SM predictions [8].

The Belle detector is designed to identify and measure particles from $\Upsilon(4S) \rightarrow B\bar{B}$ decays [9]. It is located at the interaction point (IP) of the KEKB accelerator in Tsukuba, Japan, which collides electrons and positrons at energies of 8 GeV and 3.5 GeV, respectively [10]. Charged particle tracking and momentum measurements are provided by a silicon vertex detector (SVD) and a helium/ethane central drift chamber (CDC). Particle identification (PID) is performed using the CDC in conjunction with an array of aerogel Cherenkov counters (ACC) and time-of-flight scintillators (TOF). Electrons and photons are identified and their energy measured by an electromagnetic calorimeter (ECL) of CsI(Tl) crystals. These detectors are within a 1.5T magnetic field provided by a superconducting solenoid. A layered iron and resistive plate counter detector outside the solenoid gives K_L/μ separation.

The primary signature of a $B \rightarrow K\eta'\gamma$ event is a high energy photon, which we reconstruct as an isolated shower in the ECL barrel ($32^\circ < \theta < 129^\circ$), with shape consistent with a single photon hypothesis and no associated charged track. Only photons within the range $1.8 \text{ GeV} < E_\gamma^* < 3.4 \text{ GeV}$ are considered, where the asterisk denotes the e^+e^- center-of-mass (CM) frame. All other photons in the analysis are required to have energies greater than 50 MeV. Contamination from η and π^0 mesons decaying to $\gamma\gamma$ is reduced using a likelihood technique based on probability density functions (PDFs) from Monte Carlo (MC) simulated data. If more than one photon in an event passes the selection, the one with the highest energy is taken.

Candidate η' mesons are reconstructed in the $\eta' \rightarrow \eta\pi^+\pi^-$ and $\eta' \rightarrow \rho^0\gamma$ modes. Here, η mesons are reconstructed as $\eta \rightarrow \gamma\gamma$ and $\eta \rightarrow \pi^+\pi^-\pi^0$, ρ^0 and K_S^0 mesons are reconstructed as $\pi^+\pi^-$ pairs, and π^0 mesons as $\gamma\gamma$ pairs. Charged kaons and pions are separated using a PID selection with an efficiency for kaons (pions) of 85% (98%) and a misidentification probability of 12% (14%). PID information combined with a measurement of the energy deposited in the ECL is used to reduce electron contamination.

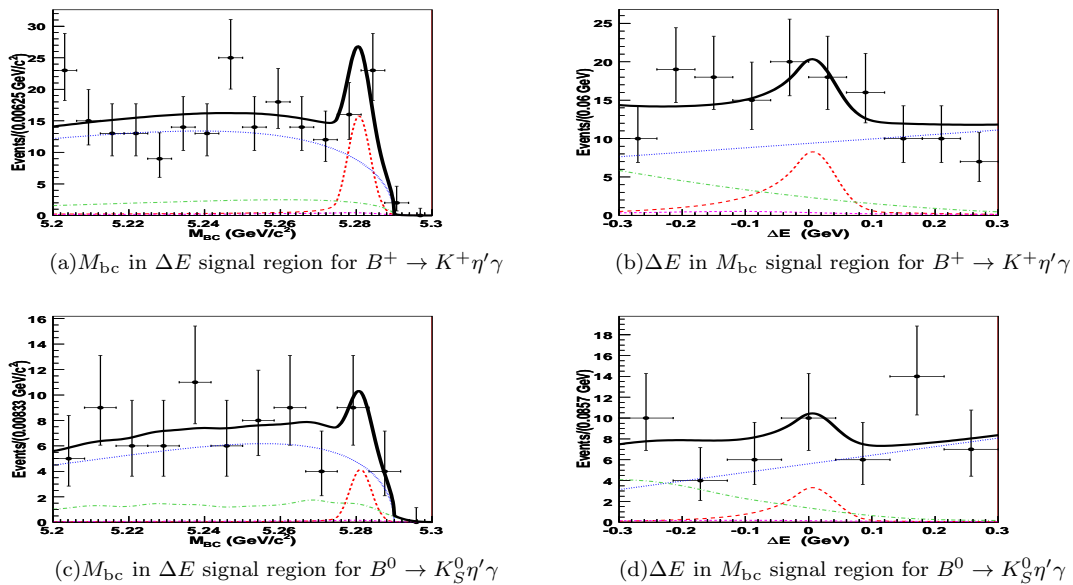


FIG. 1: Projections to the signal region from the fits to 605fb^{-1} of data. The solid lines are the combined background plus $K\eta'\gamma$ functions, the dotted lines are the $e^+e^- \rightarrow q\bar{q}$ functions, the dot-dashed the $b \rightarrow c$ functions, the long dashed the $K\eta'\gamma$ functions and the short dashed the $b \rightarrow u, d, s$ functions.

K_S^0 candidates must pass a set of momentum-dependent selection criteria based on proximity to the IP, flight length, and the angle between the momentum vector and reconstructed vertex vector. Candidates with invariant masses $10\text{MeV}c^2$ or more from the nominal K_S^0 mass of $497.7\text{MeV}c^2$ [11] are rejected, where the allowed range is equivalent to a window of 4 standard deviations (σ) of the natural mass width convolved with detector mass resolution. Neutral pion candidates must have momenta greater than $100\text{MeV}c$ and $\gamma\gamma$ combined invariant masses in the range $119\text{MeV}c^2 (2.5\sigma) < M_{\gamma\gamma} < 152\text{MeV}c^2 (3\sigma)$.

$\eta \rightarrow \gamma\gamma$ candidates are reconstructed using photons of energy greater than 100MeV , and must have invariant masses in the range $490\text{MeV}c^2 (4\sigma) < M_{\gamma\gamma} < 590\text{MeV}c^2 (3\sigma)$. They are also required to satisfy the helicity angle requirement $|\cos\theta_{\text{hel}}| < 0.9$, where θ_{hel} is the angle between the momentum vectors of the η' and one of the decay γ 's in the η rest frame. $\eta \rightarrow \pi^+\pi^-\pi^0$ candidates must have invariant masses in the range $536\text{MeV}c^2 (3\sigma) < M_{\pi^+\pi^-\pi^0} < 560\text{MeV}c^2 (3\sigma)$. The momenta of all η candidates are then corrected using a mass-constrained fit. ρ^0 candidates must have invariant masses within the range $550\text{MeV}c^2 (3\sigma) < M_{\pi^+\pi^-} < 950\text{MeV}c^2 (3\sigma)$ and also pass a helicity requirement similar to the η . A fit constraining the $\pi^+\pi^-$ vectors to a common vertex must succeed.

$\eta' \rightarrow \rho^0\gamma$ candidates must have invariant masses in the range $945\text{MeV}c^2 (2\sigma) < M_{\rho^0\gamma} < 970\text{MeV}c^2 (2\sigma)$, and the photon must have energy greater than 200MeV . $\eta' \rightarrow \eta\pi^+\pi^-$ candidates must have invariant masses within the range $950\text{MeV}c^2 (2\sigma) < M_{\eta\pi^+\pi^-} < 965\text{MeV}c^2 (2\sigma)$. Both types of candidates are required to have momenta greater than $1.0\text{GeV}c$ as measured in the CM frame.

The invariant mass of the $K\eta'$ system ($M_{K\eta'}$) is required to be less than $3.4\text{GeV}c^2$. This requirement removes some background while retaining most of the expected $M_{K\eta'}$ spectrum. Two kinematic variables are defined: $M_{bc} \equiv (1/c^2)\sqrt{E_{\text{beam}}^2 - (\vec{p}_{K\eta'}^* + \vec{p}_\gamma^*)^2 c^2}$ and $\Delta E \equiv E_B^* - E_{\text{beam}}$, where E_B^* is the energy of the candidate B meson in the CM frame, E_{beam} is half the total CM energy ($\sqrt{s}/2$), and $\vec{p}_{K\eta'}^*$ and \vec{p}_γ^* are the CM frame momenta of the $K\eta'$ combination and the signal photon, respectively. In the calculation of M_{bc} , the momentum of the signal photon is rescaled to be $p_\gamma^* = (1/c)(E_{\text{beam}} - E_{K\eta'}^*)$. B candidates must satisfy $|\Delta E| < 0.3\text{GeV}$ and $5.20\text{GeV}c^2 < M_{bc} < 5.29\text{GeV}c^2$, and the signal region is defined as $-0.1\text{GeV} < \Delta E < 0.07\text{GeV}$ and $5.27\text{GeV}c^2 < M_{bc} < 5.29\text{GeV}c^2$.

Backgrounds to $K\eta'\gamma$ events are estimated using large MC samples [12]. The dominant background is from $e^+e^- \rightarrow q\bar{q}$ ($q = u, d, s, c$) continuum processes. To reduce this we form a Fisher discriminant [13] from 16 modified Fox-Wolfram moments [14] and the scalar sum of the event transverse momenta. A likelihood ratio (LR) is formed from the optimized Fisher discriminant, the cosine of the angle between the B meson flight direction and the positron beam axis, and the distance along the positron beam axis between the two B meson vertices, which are reconstructed from the SVD and CDC response to charged particles. The signal regions of the LR distributions are chosen by maximizing the figure of merit defined as $\mathcal{N}_S/(\sqrt{\mathcal{N}_S + \mathcal{N}_{SB}})$, where \mathcal{N}_S is the number of $B \rightarrow K\eta'\gamma$ MC events that lie above a certain LR value and \mathcal{N}_{SB} is the corresponding number of sideband data events lying above the same value. The

TABLE I: The yields, efficiencies (ε), daughter branching fraction products (Π), measured branching fractions (\mathcal{B}), signal significances including systematics (\mathcal{S}) and 90% CL ULs for the measured decays.

Mode	Yield(events)	ε	Π	$\mathcal{B}(10^{-6})$	$\mathcal{S}(\sigma)$	UL(10^{-6})
$B^+ \rightarrow K^+ \eta' \gamma$	$32.6^{+11.8}_{-10.8}$	0.024	0.571	$3.6 \pm 1.2 \pm 0.4$	3.3	5.6
$B^0 \rightarrow K^0 \eta' \gamma$	$5.1^{+5.0}_{-4.0}$	0.016	0.197	$2.5^{+2.4+0.4}_{-1.9-0.5}$	1.3	6.4

data sideband regions are defined as $M_{bc} < 5.26 \text{ GeV}/c^2$ and either $\Delta E < -0.2 \text{ GeV}$ or $\Delta E > 0.1 \text{ GeV}$. The BF central values found in the BABAR $K\eta'\gamma$ analysis [3] are used to calculate \mathcal{N}_S , and the sideband data is scaled by the ratio of $q\bar{q}$ MC events in the full fitting region to those in the sideband region. To maximize discrimination, the optimization of the figure of merit is performed in bins of flavour-tagging quality, as calculated by the Belle B -flavour tagging algorithm [15]. The LR requirements are 38% efficient for signal MC and remove 98% of background.

A significant proportion of the MC events modelled as $b \rightarrow c$ processes that pass the above selection criteria are found to include a D^0 meson. Any kaon candidate which forms an invariant mass within the range $1.84 \text{ GeV}/c^2 < M_{K-\pi^+} < 1.89 \text{ GeV}/c^2$ when combined with any charged pion in the same event is removed from consideration, in order to suppress $D^0 \rightarrow K^-\pi^+$ decays. $B \rightarrow J/\psi K \rightarrow (\eta'\gamma)K$ events are suppressed by vetoing candidates with a combined $\eta'\gamma$ invariant mass within $\pm 25 \text{ MeV}/c^2$ of the nominal J/ψ mass [11]. This reduces this background to a negligible level.

On average, 1.24 candidates per signal MC event pass the selection criteria. A series of selection criteria are used to choose the best candidate, including the lowest B vertex χ^2 , the lowest $\rho^0 \rightarrow \pi^+\pi^-$ or $\eta' \rightarrow \eta\pi^+\pi^-$ vertex χ^2 , the reconstruction with η candidate invariant mass closest to the nominal value [11], the highest E_γ from $\eta' \rightarrow \rho^0\gamma$, and the lowest K_S^0 vertex χ^2 . This technique selects the correct candidate in 76% of cases.

Signal yields are extracted using extended unbinned maximum likelihood fits to ΔE and M_{bc} . All reconstructed charged final states are combined into one fitted distribution, and all reconstructed neutral final states are combined into another. PDF parameters are determined from MC distributions. The $K\eta'\gamma$ distribution is modelled with a Crystal Ball line shape (CBLS) [16] function for M_{bc} and CBLS plus Gaussian functions with common means and relative widths for ΔE . The $b \rightarrow c$ background is modelled with an ARGUS [17] function for M_{bc} and a second order Chebyshev polynomial for ΔE . The $b \rightarrow u, d, s$ background is modelled with a 2D Keys PDF [18]. The $e^+e^- \rightarrow q\bar{q}$ distribution is modelled with an ARGUS function for M_{bc} and a first order Chebyshev polynomial for ΔE .

The means and widths of the CBLS functions describing the $K\eta'\gamma$ distribution in ΔE and M_{bc} are calibrated using large control samples of $B \rightarrow K^*(892)\gamma$ data and MC. The PDFs of the $K\eta'\gamma$, $e^+e^- \rightarrow q\bar{q}$, $b \rightarrow c$ and $b \rightarrow u, d, s$ distributions are combined and used to fit the 605 fb^{-1} of accumulated data. The normalizations of the $b \rightarrow c$ and $b \rightarrow u, d, s$ components are fixed to values expected from MC studies; the $K\eta'\gamma$ and $e^+e^- \rightarrow q\bar{q}$ normalizations and the $e^+e^- \rightarrow q\bar{q}$ function parameters are allowed to float, except for the ARGUS endpoint, which is fixed to $5.29 \text{ GeV}/c^2$. Figure 1 shows the results of the $B^+ \rightarrow K^+\eta'\gamma$ and $B^0 \rightarrow K_S^0\eta'\gamma$ fits to data, where the M_{bc} plots show a projection in the ΔE signal region and the ΔE plots show a projection in the M_{bc} signal region.

Table I shows the measured yields and signal significances for the fits to data. We find 33^{+12}_{-11} events for the fit to the charged modes and 5^{+5}_{-4} events for the fit to the neutral modes. The signal significance is defined as $\sqrt{-2\ln(L_0/L_{\max})}$, where L_{\max} and L_0 are the values of the likelihood function when the signal yield is floated or fixed to zero, respectively. The systematic errors described below are included in the significances by convolving the likelihood functions with Gaussians of width defined by the magnitude of the errors. The signal significances including systematic errors are 3.3σ and 1.3σ for the charged modes and neutral modes, respectively.

Any bias in the fitting process is determined using pseudoexperiments of MC scaled to the yields returned by the fits to data. The $e^+e^- \rightarrow q\bar{q}$ and $b \rightarrow c$ MC components are generated from the shape of the PDFs and combined with fully simulated MC for the $K\eta'\gamma$ and $b \rightarrow u, d, s$ components. The analysis of 1000 pseudoexperiments finds no significant bias.

The signal MC reconstruction efficiencies are calculated as the number of $K\eta'\gamma$ events passing the selection criteria divided by the number generated. To calibrate for $M_{K\eta'}$ dependence, the efficiencies in 10 bins across $M_{K\eta'}$ are weighted according to the efficiency-corrected background-subtracted $M_{K\eta'}$ distributions in data. The means of these weighted efficiencies are listed in the ε column of Table I.

The BFs are calculated from the signal yields, calibrated efficiencies, daughter BF products, and the number of B mesons in the data sample. Equal production of charged and neutral B meson pairs is assumed. We find $\mathcal{B}(B^+ \rightarrow K^+\eta'\gamma) = (3.6 \pm 1.2 \pm 0.4) \times 10^{-6}$ and $\mathcal{B}(B^0 \rightarrow K^0\eta'\gamma) = (2.5^{+2.4+0.4}_{-1.9-0.5}) \times 10^{-6}$, where the first errors are statistical and the second systematic. The 90% CL ULs are found to be $\mathcal{B}(B^+ \rightarrow K^+\eta'\gamma) < 5.6 \times 10^{-6}$, and $\mathcal{B}(B^0 \rightarrow K^0\eta'\gamma) < 6.4 \times 10^{-6}$. The ULs are calculated by integrating the likelihood function with systematic errors included in the physically allowed BF region. The UL is then defined as the BF below which 90% of the integrated

likelihood lies. The BF's and ULs are measured within the reduced phase-space region $M_{K\eta'} < 3.4 \text{ GeV}/c^2$.

The systematic uncertainties for the charged (neutral) BF include errors on the following processes: photon detection (2.8% (2.8%)); π^0 reconstruction (0.8% (0.5%)); K_S^0 reconstruction (0.0% (4.5%)); η reconstruction (3.4% (3.6%)); charged track detection (3.8% (5.0%)); K^+/π^+ differentiation (1.4% (1.5%)); and the calculated number of $B\bar{B}$ pairs in the data sample (1.4% (1.4%)). The statistical uncertainty on the MC efficiency after calibration is 1.7% (1.9%). The data/MC LR selection efficiency difference is estimated to be 3.7%(3.7%) using a $B \rightarrow K^*(892)\gamma$ control sample. The vetoes on $M_{\eta'\gamma}$ around the J/ψ invariant mass and on $M_{K-\pi^+}$ around the D^0 mass are found to affect the reconstruction efficiency by 0.2% (0.4%) and 0.5% (0.0%) respectively. The bias study results have an uncertainty of 1.5% (3.5%). The correction of the signal reconstruction efficiency from the $M_{K\eta'}$ distributions has an uncertainty of 1.2% (1.5%). The effect of $K_S^0\eta'\gamma$ events being reconstructed as $K^+\eta'\gamma$ and entering the incorrect fit distribution, and *vice versa*, gives a $-6\%(+6\%)$ efficiency uncertainty. All fixed parameters in the fit to data are varied by $\pm 1\sigma$ (the $b \rightarrow c$ and $b \rightarrow u, d, s$ yields by 3σ), yielding uncertainties of $(+6.5\%, -6.7\%)$ for $B^+ \rightarrow K^+\eta'\gamma$, and $(+11.7\%, -16.6\%)$ for $B^0 \rightarrow K_S^0\eta'\gamma$.

The existing measurements of $B \rightarrow X_s\gamma$ and $B \rightarrow X_sl^+l^-$ both rely heavily on the accuracy of the X_s hadronization model performed by the JETSET [19] program [20][21][22]. A large sample of inclusive $B \rightarrow X_s\gamma$ MC was generated with the X_s system hadronized by JETSET according to the Kagan-Neubert model [23] and the mass of the b quark set to $4.75 \text{ GeV}/c^2$. From this sample, the model predicts the BF of $B^+ \rightarrow K^+\eta'\gamma$ events in the region $M_{K\eta'} < 3.4 \text{ GeV}/c^2$ to be $(1.8 \pm 0.2) \times 10^{-6}$, while we measure $(3.6 \pm 1.2 \pm 0.4) \times 10^{-6}$. In addition, this model predicts $\mathcal{B}(B \rightarrow K\eta\gamma)$ to be $(8.2 \pm 0.9) \times 10^{-6}$ using the same sample, which can be compared to the measured BF of $(7.9 \pm 0.9) \times 10^{-6}$ [11]. With the current statistics, the BF's for both $B^+ \rightarrow K^+\eta'\gamma$ and $B \rightarrow K\eta\gamma$ are consistent with the Kagan-Neubert model.

In conclusion, we report the first evidence of the decay $B^+ \rightarrow K^+\eta'\gamma$ with a partial BF of $\mathcal{B}(B^+ \rightarrow K^+\eta'\gamma) = (3.6 \pm 1.2 \pm 0.4) \times 10^{-6}$ and a significance of 3.3σ in the region $M_{K\eta'} < 3.4 \text{ GeV}/c^2$. We also set a 90% CL UL of $\mathcal{B}(B^0 \rightarrow K^0\eta'\gamma) < 6.4 \times 10^{-6}$ in the same $M_{K\eta'}$ region.

We thank the KEKB group for excellent operation of the accelerator, the KEK cryogenics group for efficient solenoid operations, and the KEK computer group and the NII for valuable computing and SINET3 network support. We acknowledge support from MEXT, JSPS and Nagoya's TLPRC (Japan); ARC and DIISR (Australia); NSFC (China); DST (India); MOEHRD and KOSEF (Korea); MNiSW (Poland); MES and RFAAE (Russia); ARRS (Slovenia); SNSF (Switzerland); NSC and MOE (Taiwan); and DOE (USA).

-
- [1] E. Barberio *et al.*, Heavy Flavour Averaging Group, hep-ex/0808.1297 (2008).
 - [2] M. Misiak *et al.*, Phys. Rev. Lett. **98**, 022002 (2007).
 - [3] B. Aubert *et al.*, BABAR Collaboration, Phys. Rev. D **74**, 031102(R) (2006).
 - [4] H. J. Lipkin, Phys. Lett. B **254**, 247 (1991).
 - [5] M. Beneke and M. Neubert, Nucl. Phys. B **651**, 225 (2003).
 - [6] S. Nishida *et al.*, Belle Collaboration, Phys. Lett. B **610**, 1 (2005).
 - [7] The charge-conjugate modes of all decays in this paper are implied unless explicitly stated otherwise.
 - [8] D. Atwood *et al.*, hep-ph/9704272v1, (1997).
 - [9] A. Abashian *et al.*, Belle Collaboration, Nucl. Instr. and Meth. A **479**, 117 (2002).
 - [10] S. Kurokawa and E. Kikutani, Nucl. Instr. and Meth. A **499**, 1 (2003), and other papers included in this volume.
 - [11] C. Amsler *et al.*, Particle Data Group, Phys. Lett. B **667**, 1 (2008).
 - [12] Events are generated with the CLEO QQ generator (see <http://www.lns.cornell.edu/public/CLEO/soft/QQ>), or the Evtgen generator: D. J. Lange, Nucl. Instrum. and Meth. Phys. Res. Sect. A **462**, 152 (2001). Detector response is simulated with GEANT: R. Brun *et al.*, GEANT 3.21, CERN Report DD/EE/84-1, 1984.
 - [13] R. A. Fisher, Annals of Eugenics **7**, 179 (1936).
 - [14] The Fox-Wolfram moments were introduced in G. C. Fox and S. Wolfram, Phys. Rev. Lett. **41**, 1581 (1978). The modified moments used in this analysis are described by S. H. Lee *et al.*, Belle Collaboration, Phys. Rev. Lett. **91**, 261801 (2003).
 - [15] H. Kakuno *et al.*, Belle Collaboration, Nucl. Instr. and Meth. A **533**, 516 (2004).
 - [16] T. Skwarnicki, Ph.D. Thesis, Institute for Nuclear Physics, Krakow (1986); DESY Internal Report, DESY F31-86-02 (1986).
 - [17] H. Albrecht *et al.*, ARGUS Collaboration, Phys. Lett. B **241**, 278 (1990).
 - [18] K. Cranmer, Comp. Phys. Comm. **136**, 198 (2001).
 - [19] T. Sjostrand, Comp. Phys. Comm. **82**, 74 (1994).
 - [20] M. Iwasaki *et al.*, Phys. Rev. D **72**, 092005 (2005).
 - [21] S. Nishida *et al.*, Phys. Rev. Lett. **93**, 031803 (2004).
 - [22] B. Aubert *et al.*, Phys. Rev. Lett. **101**, 171804 (2008).
 - [23] A. L. Kagan and M. Neubert, Eur. Phys. J. C **7**, 5 (1999).